



**University of
Zurich**^{UZH}

**Zurich Open Repository and
Archive**

University of Zurich
University Library
Strickhofstrasse 39
CH-8057 Zurich
www.zora.uzh.ch

Year: 2014

Inflammatory response of lung macrophages and epithelial cells after exposure to redox active nanoparticles: Effect of solubility and antioxidant treatment

Urner, Martin ; Schlicker, Andreas ; Z'graggen, Birgit Roth ; Stepuk, Alexander ; Booy, Christa ; Buehler, Karl P ; Limbach, Ludwig ; Chmiel, Corinne ; Stark, Wendelin J ; Beck-Schimmer, Beatrice

DOI: <https://doi.org/10.1021/es504011m>

Posted at the Zurich Open Repository and Archive, University of Zurich

ZORA URL: <https://doi.org/10.5167/uzh-106757>

Journal Article

Accepted Version

Originally published at:

Urner, Martin; Schlicker, Andreas; Z'graggen, Birgit Roth; Stepuk, Alexander; Booy, Christa; Buehler, Karl P; Limbach, Ludwig; Chmiel, Corinne; Stark, Wendelin J; Beck-Schimmer, Beatrice (2014). Inflammatory response of lung macrophages and epithelial cells after exposure to redox active nanoparticles: Effect of solubility and antioxidant treatment. *Environmental Science Technology*, 48(23):13960-13968.

DOI: <https://doi.org/10.1021/es504011m>

Inflammatory response of lung macrophages and epithelial cells after exposure to redox active nanoparticles: Effect of solubility and antioxidant treatment

Martin Urner^{◦, ‡}, Andreas Schlicker^{◦, ‡}, Birgit Roth Z'graggen[◦], Alexander Stepuk[§], Christa Booy[◦], Karl P. Buehler[◦], Ludwig Limbach[§], Corinne Chmiel[†], Wendelin J. Stark^{§, X}, and Beatrice Beck-Schimmer^{, ◦, X}*

[◦] Institute of Anesthesiology, University Hospital Zurich, 8091 Zurich, Switzerland; Institute of Physiology, Zurich Center for Integrative Human Physiology, University of Zurich, 8057 Zurich, Switzerland.

[§] Institute for Chemical and Bioengineering, Department of Chemistry and Applied Biosciences, ETH Zurich, 8093 Zurich, Switzerland.

[†] Institute of General Practice and Health Services Research, University of Zurich, 8091 Zürich, Switzerland

KEYWORDS: Metal oxide nanoparticles, reactive oxygen species, inflammation, cell viability, effector cells, target cells

ABSTRACT

The effects of an exposure to three mass-produced metal oxide nanoparticles – similar in size and specific surface area, but different in redox activity and solubility – were studied in rat alveolar macrophages (MAC) and epithelial cells (AEC). We hypothesized that the cell response depends on the particle redox activity and solubility determining the amount of reactive oxygen species formation (ROS) and subsequent inflammatory response. MAC and AEC were exposed to different amounts of Mn_3O_4 (soluble, redox-active), CeO_2 (insoluble, redox-active), and TiO_2 (insoluble, redox-inert) up to 24 hours. Viability and inflammatory response were monitored with and without co-incubation of a free-radical scavenger (trolox). In MAC elevated ROS levels, decreased metabolic activity and attenuated inflammatory mediator secretion were observed in response to Mn_3O_4 . Addition of trolox partially resolved these changes. In AEC, decreased metabolic activity and an attenuated inflammatory mediator secretion were found in response to CeO_2 exposure without increased production of ROS, thus not sensitive to trolox administration. Interestingly, highly redox-active soluble particles did not provoke an inflammatory response. The data reveal that target and effector cells of the lung react in different ways to particle exposure making a prediction of the response depending from redox activity and intracellular solubility difficult.

INTRODUCTION

Metal oxide nanoparticles are an important class of nanomaterial with an annual production rate reaching the megatons. Present and future opportunities include a wide range of applications in water purification and environmental technology (cerium dioxide)¹, metal oxide particles as additives in consumer products (titanium dioxide)², or in the manufacturing process of dry cell batteries³ and as fungicides (manganese oxide)⁴. The widespread use comes along with the environmental burden and potentially dangerous human exposure.

Therefore, thorough evaluation and understanding of the potential risks that metal oxide nanoparticles might pose to human health is of utmost importance. As the main route of accidental exposure to humans occurs by inhalation the interaction of metal oxide nanoparticles with cells of the alveolar compartment is of high interest. While titanium and cerium oxides have a low toxicity profile manganese is an essential metal with a high toxicological concern. It is well known that exposure to metal particles such as metal fume with oxides as major component can cause acute respiratory symptoms in exposed workers. However, pulmonary effects are usually mild and reversible in healthy people ⁵⁻⁷. Observational reports suggest an increased incidence of mortality from pneumonia among welders after exposure to metal fumes ^{8,9}.

In the present study, the response of alveolar macrophages (MAC) and alveolar epithelial cells (AEC) as main effector and target cells of the respiratory compartment on exposure to three different, well-characterized metal oxide nanoparticles was evaluated: manganese oxide (Mn_3O_4), a partially soluble metal oxide nanoparticle, as well as two insoluble ceramic nanomaterials – titanium dioxide (TiO_2), and cerium oxide (CeO_2). While TiO_2 particles are redox-inert, Mn_3O_4 and CeO_2 particles are both redox-active. The particles are comparable regarding morphology, size, shape, and degree of agglomeration, but differ in redox activity and intracellular solubility¹⁰. The particle concentration in the experiments was set within the range of 1 to 6 μg per cm^2 cell surface (corresponds to 5 to 20 $\text{mg} \cdot \text{kg}^{-1}$ cell culture media), in analogy to previous published data with these particles¹¹. The chosen amounts of particles may simulate an exposure scenario during particle synthesis¹². We hypothesized that viability and response of MAC and AEC depend on the particles' redox activity and intracellular solubility determining the amount of oxidative stress and reactive oxygen species (ROS) formation in cells. We additionally assumed that due to particle-induced intracellular production of ROS an inflammatory reaction in these cells of the alveolar compartment is provoked, especially upon exposure to Mn_3O_4 . As an important cytokine within the

orchestration of an inflammatory reaction – not only recruiting macrophages but also neutrophils - monocyte chemoattractant protein-1 (MCP-1) was assessed in the supernatants of MAC and AEC.

MATERIALS AND METHODS

Nanoparticle characterization and preparation. All experiments were performed using Mn_3O_4 , CeO_2 and TiO_2 particles at a concentration of 20 mg kg^{-1} in the assay medium.

The phase composition of flame-spray prepared material was characterized by X-ray diffraction (XRD) patterns recorded on a PANalytical XPert PRO-MPD (CuK α radiation, X'Celerator linear detector system, step size of 0.033° , ambient conditions). Brunauer-Emmett-Teller (BET) method was used for analysis of the specific surface area by measuring the nitrogen adsorption at 77 K on a Tristar (Micromeritics Instruments). Prior the analysis, samples were preheated at 150°C with $p < 0.1 \text{ mbar}$ during 1 hour. The size and morphology of the prepared nanoparticles were characterized by transmission electron microscopy (TEM) on a Philips CM30 ST (LaB $_6$ cathode, operated at 300 kV, point resolution 4 Å). The composition of nanoparticle-containing medium solutions was characterized by inductively coupled plasma optical emission spectroscopy (ICP OES, Horiba Ultra 2). A detailed description of the nanoparticle preparation is given elsewhere¹¹. More detailed information is enclosed in the supporting information.

Cells and culture conditions. The rat MAC cell line CRL-2192 and rat AEC cell line CCL-149 were purchased from American Type Culture Collection (Manassas, VA, USA) and cultured as described in ¹³ and ¹⁴. A defined cell number of 150'000 MAC or 300'000 AEC was seeded in 24-well polystyrene plates (Costar®, Corning Int., Corning, NY, USA). For treatment cells were exposed to medium containing 5 to 20 mg kg^{-1} of metal oxide particles or medium alone (=control group) over time periods of 4 hours, 8 hours or 24 hours (1 to 6 μg

particles per cm² cell surface). As in previous studies, reduced serum concentrations (1%) were used during exposure ¹¹.

Determination of oxidative stress. Reactive oxygen species formation was measured assessing the oxidation of non-fluorescent 2',7'-dichlorofluorescein-diacetate (=DCFH-DA) to the fluorescent DCF ^{11, 15, 16}. Values of untreated control cells (=reference group) were defined as 100% to evaluate the results. SIN-1 (3-morpholinopyrrolidine hydrochloride; Sigma-Aldrich, Buchs, Switzerland), a ROS generating agent, was used at a concentration of 200µM as positive control ¹⁷. Detailed description of the experimental procedure is described in the supporting information.

Viability and cytotoxicity tests. The tetrazolium bromide (MTT) assay, determining the amount of NADPH oxidase-related metabolic activity, was used to measure the cells' viability in vitro ¹⁸. Changes in amount of DNA were monitored according to a previous publication ¹⁹ using Hoechst 33258 reagent (Sigma-Aldrich, Buchs, Switzerland). Both assays have already successfully been used in cells exposed to metal oxide particles to observe potential cytotoxicity ²⁰. The apoptosis rate of cells was determined using fluorometric assays for the measurement of caspase-3 activity ²¹. To evaluate the results, untreated control cells were defined as the reference category (=100%). We used Ac-Asp-Glu-Val-Asp-H (Aldehyde) (from PeptaNova, Sandhausen, Germany) at a concentration of 100µM as caspase-3 inhibitor.

Determination of the inflammatory response. To measure MCP-1 protein in the supernatants of MAC and AEC, enzyme-linked immunosorbent assays (ELISA) were performed according to the manufacturer's recommendations, using OptEIA™ rat MCP-1 ELISA (BD Biosciences Pharmingen, San Diego, CA, USA). Optical density was determined at 492 nm and the results were given in pg/mL. Lower detection limits of the MCP-1 ELISA were at 30 pg/mL. We also measured cytokine-induced neutrophil chemoattractant protein-1 (CINC-1) by ELISA technique (R&D Systems Europe Ltd., Abingdon, United Kingdom), as

well as tumor necrosis factor- α (TNF- α) protein (TNF- α ELISA, BD Biosciences, San Diego, CA, USA). Both assays have a lower detection limit of 15 pg/mL.

ROS binding experiments. 6-hydroxy-2, 5, 7, 8-tetramethylchroman-2-carboxylic acid (trolox, Sigma-Aldrich, Buchs, Switzerland) is a water-soluble vitamin E derivative with strong antioxidant properties which was used in our experiments at concentrations of 200 μ M solved in the cell culture medium to act as free-radical scavenger. Trolox was co-incubated with the according nanoparticles.

Statistical analysis. SPSS Version 20 (SPSS Inc, Chicago, Ill) was used to perform all statistical analyses. All experiments were at least performed 3 times each with six independent samples per group. Linear regression was used to evaluate the influence of metal oxide particle exposure on MAC and AEC. Unexposed control cells were used as reference category. Metal oxide particle exposures (Mn_3O_4 , CeO_2 , TiO_2), the treatment with trolox, and the different measurement timepoints were included as independent predictors in the linear regression models. For all analyses, we considered $p < 0.05$ to be statistically significant. See supporting information for a more detailed description of the procedures.

RESULTS

Nanoparticles characterization. The nanoparticles of Mn_3O_4 , CeO_2 and TiO_2 were prepared by flame-spray pyrolysis. Based on the X-ray diffraction patterns Mn_3O_4 and CeO_2 showed monophasic composition with characteristic peaks corresponding to hausmannite and cerium dioxide, respectively. TiO_2 nanoparticles revealed two phases: rutile and anatase (**Figure 1A**). Mn_3O_4 nanoparticles have the largest specific surface area of $61 \text{ m}^2 * \text{g}^{-1}$ corresponding to smaller particle sizes of 20 nm as measured by BET (**Supplementary Table S1**). Titanium oxide and cerium dioxide consisted of nanoparticles with sizes of 33 and 23 nm, respectively. TEM micrographs showed Mn_3O_4 agglomerates of submicron size, consisting of

approximately 30 nm nanoparticles, which correlates well with the data acquired from BET measurements (**Figure 1B and 1C**). Using ICP-OES the metal content was analyzed in collected cell lysates (**Figures 1D and 1E**) and in the supernatants. In the cell lysates of MAC, cerium continuously increased over time, while manganese, after reaching an early plateau slightly decreased (**Figure 1D**). In AEC, cerium measurements peaked at a very early time point of 4 h, followed by a continuous decrease of concentration, while the amount of manganese rose steadily in a time-dependent manner (**Figure 1E**). Traces of titanium were below detection limit (LOD = 2 ppb) in lysates of both MAC and AEC. In the supernatants, we observed for cerium decreasing, but rather constant concentrations over the duration of the experiments following a time-dependent profile (**Supplementary Figure S1**). For manganese, we measured slightly higher levels in supernatants of AEC, while a time-dependent increase in concentration was observed in the supernatant of both cell types (**Supplementary Figure S1**). Titanium remained also in the supernatants below detection limit (LOD = 2 ppb).

Generation of ROS in response to metal oxide exposure. Assuming that exposure to the three metal oxide nanoparticles induces different amounts of oxidative stress we measured ROS formation in MAC and AEC in relation to unexposed control cells. Overall, remarkably more ROS were formed in MAC compared to AEC. In both cell types a significant change over time was observed (both p-values <0.001, **Figure 2A and 2B**). The overall raise in concentration of ROS was most pronounced when cells were exposed to Mn₃O₄ particles (both p-values <0.001, **Supplementary Table S2**). Compared to the unexposed control cells (defined as 100%), the amount of ROS in MAC was increased by +346% after 24 hours, while in AEC an increase of +84% was measured. All ROS results generated in incubation with Mn₃O₄ particles were corrected by subtraction using the results from cell-free assays (background subtraction). This was due to a dose-dependent oxidation of DCFH to DCF

which was found in cell-free experiments upon addition of Mn_3O_4 particles (spearman's rho: 0.969, $p < 0.001$). CeO_2 or TiO_2 particles had no effect on DCFH.

NADPH oxidase-related metabolic activity and cell survival. The influence of the particles on cellular NADPH oxidase-related metabolic activity and the amount of DNA is described in **Supplementary Table S2**. In MAC, NADPH oxidase-related metabolic activity decreased time- and dose-dependently when incubated with Mn_3O_4 particles ($p < 0.001$, **Figure 3A and 3B**). This was not observed for CeO_2 and TiO_2 particles. After 24 hours, NADPH oxidase-related metabolic activity levels of Mn_3O_4 -exposed MAC were reduced by 68%. Mn_3O_4 , CeO_2 , and TiO_2 particles had no significant effect on the amount of DNA (**Supplementary Figure S2**). In AEC, however, NADPH oxidase-related metabolic activity was not influenced by Mn_3O_4 particle exposure, but dose-dependently reduced after CeO_2 and TiO_2 particles exposure (**Figure 3C and 3D**; rho: -0.297, $p = 0.005$ for CeO_2 and rho: -0.280, $p = 0.008$ for TiO_2 , respectively). As for MAC no particle-induced changes in the amount of DNA were found in AEC after incubation with the three metal oxides (**Supplementary Figure S2**). Inaccuracies of measurements due to interactions of nanoparticles with the viability or DNA quantification assays were measured below 15%.

Inflammatory response in alveolar macrophages (MAC) and alveolar epithelial cells (AEC). As marker of inflammatory response, MCP-1 protein was assessed after 4, 8, and 24 hours of exposure to metal oxide particles (**Supplementary Table S2**). In both, MAC and AEC, MCP-1 protein expression was gradually increased with the duration of incubation – representing basal secretion without interaction with nanoparticles. In MAC, a dose-dependent decrease of MCP-1 protein expression in response to Mn_3O_4 was found (rho: -0.367, $p < 0.001$). MCP-1 protein expression was attenuated by 9658 pg/mL (mean of the 3 time points 4, 8 and 24 hours) when exposed to Mn_3O_4 particles (**Figure 4A and 4B**). No significant influence of CeO_2 or TiO_2 particle exposure on MCP-1 protein expression was detected. In AEC, a decreased MCP-1 protein expression was measured by 781 pg/mL after

exposure to Mn_3O_4 (**Figure 4B**), and by 1675 pg/mL in incubation with CeO_2 particles (mean of the 3 time points). In AEC dose-dependency of this effect could only be shown for CeO_2 particles (ρ : -0.288, $p < 0.001$), but not for Mn_3O_4 particle exposure ($p = 0.24$).

Determined MCP-1 protein levels in supernatants were not in correlation ($p = 0.239$) with the metal oxides potential to adsorb inflammatory mediators (**Supplementary Figure S3**). We also measured other cytokines, such as CINC-1 protein expression in AEC and $TNF-\alpha$ secretion in MAC, but the levels in the supernatants were below the detection limit of the respective assays.

Mechanism of impaired NADPH oxidase-related metabolic activity and attenuated inflammatory mediator secretion. Expression of MCP-1 protein significantly correlated with the amount of intracellular ROS in MAC (ρ : -0.346, $p < 0.001$). Using the vitamin E derivative trolox, we tried to impact on elevated ROS levels in Mn_3O_4 -exposed MAC (**Figure 5A**). When cells were co-incubated with trolox, the amount of ROS (mean of the 3 time points) was reduced 4-fold compared to an exposure with Mn_3O_4 particles solely ($p < 0.05$, **Supplementary Table S3**). Also impaired NADPH oxidase-related metabolic activity in Mn_3O_4 -exposed MAC was partially restored by addition of trolox to the culture medium ($p < 0.001$, **Figure 5B**). Compared to sole exposure to Mn_3O_4 particles, NADPH oxidase-related metabolic activity was +13% higher (mean of 3 time points) when MAC were additionally treated with trolox. As described above, the amount of DNA was not changed by Mn_3O_4 particle exposure. Earlier work, however, reported increased apoptosis rate in AEC as response to Mn_3O_4 particle exposure¹¹. We therefore assessed caspase-3 activity in MAC with and without the presence of trolox (**Figure 5C**). A Mn_3O_4 -induced up-regulation of caspase-3 activity of about +50% was found (mean of 3 time points). This increase was partially attenuated by treatment of MAC with trolox. The Mn_3O_4 -induced up-regulation of caspase-3 activity was also abolished when a caspase-3 inhibitor was added to the cell-culture medium (**Supplementary Figure S4**). In accordance with the attenuated caspase-3 activity

and the recovered NADPH oxidase-related metabolic activity, the secretion of inflammatory mediators was completely restored in Mn₃O₄-exposed MAC, when trolox was added to the culture medium (p<0.05, **Figure 5D, Supplementary Table S3**). In contrast to the findings described for MAC, the amount of intracellular ROS did not correlate with decreased MCP-1 protein secretion in AEC (p=0.262). The compromised NADPH oxidase-related metabolic activity in AEC was not correlated with attenuated MCP-1 protein secretion (p=0.375). No effect of trolox on NADPH oxidase-related metabolic activity (overall p=0.685) or on reduced MCP-1 secretion (overall p=0.566) could be observed in AEC (**Supplementary Figure S5**).

DISCUSSION

Accidental occupational exposure to metal fume can provoke a broad range of acute respiratory symptoms and systemic reactions such as metal fume fever^{5-7, 22, 23}. In this study, we investigated the effect of three representative metal oxide nanoparticles on effector and target cells of the alveolar compartment, namely MAC and AEC. Exposure to redox-inert and insoluble material, such as TiO₂, had only marginal effect on intracellular ROS levels, viability and inflammatory mediator expression in MAC and AEC. Mn₃O₄ as partially intracellular soluble and redox-active material – provoked in MAC highly increased ROS levels, but suppressed production of inflammatory mediators at the same time. These findings were completely reversible by addition of a free radical scavenger. In AEC, only marginal ROS formation was observed in the presence of Mn₃O₄. In this cell-type, NADPH oxidase-related metabolic activity and production of inflammatory mediators were particularly impaired by CeO₂ – interestingly in a ROS-independent way. The observation of a cell type-specific response to particle exposure is not surprising with regard to the given differences in anatomy and physiology of MAC and AEC (e.g. the amount of intracellular lysosomes). Our findings are in contrast to a previous publication describing a predictive paradigm for

oxidative stress and pulmonary inflammation²⁴. Though, these experiments were performed in other cell lines and under different cell culture conditions and can therefore not be compared. Some cell types might be more sensitive compared to others. This is illustrated in the work of Cronholm et al.²⁵ in which different results with regard to cytotoxicity have been found comparing the human lung cell lines A549 and BEAS-2B. Also Semisch et al.²⁶ found differences in the investigated cell types in response to exposure to the same nanoparticles (A549 and HeLa S3 cells). Numerous reasons such as interspecies differences, epigenetic changes (e.g. due to culturing the cells) or different amounts of intracellular antioxidants may account for different observations in cells after exposure to the same nanomaterial.

Dissolution and uptake of particles

With regard to the results from ICP-OES analysis, two mechanisms can eliminate metal from the supernatants: nanoparticle agglomeration and subsequent sedimentation²⁷ leading to larger agglomerates sticking to the bottom of the cell culture well (irreversibly lost, not recovered during further analysis), or uptake into the cells (recovered within the cell lysate). The observed concentration profile of cerium in supernatants of both cell types may be either the result of good dispersion stability, or formation of soluble cerium species. The used chemical analysis of the metal content is very accurate, but cannot distinguish the species present (particulate, oxide or dissolved ions). Levels of titanium remained below detection limit. Hence, all TiO₂ nanoparticles finally ended up in a non-detectable form: i.e. either as large agglomerates sticking to the bottom of cell culture dishes, or large agglomerates removed after sample collection. In contrast to the previous two insoluble materials, Mn₃O₄ particles are able to slowly dissolve and thereby form soluble manganese ions that can freely float in the supernatant. The difference in manganese concentrations observed in supernatants of MAC and AEC, might relate to different amounts of Mn₃O₄ dissolution, which might be promoted by common metabolic by-products, such as small carboxylic acids or metal

chelators, secreted by cells in response to metal exposure (**Supplementary Figure S1**). The observed concentration range suggests a significant contribution from dissolution (several mg kg⁻¹ manganese were detected). However, agglomeration and sedimentation with subsequent sticking to cell culture dish surfaces is most probably responsible for the difference between analyzed manganese (sum of manganese found in the supernatant and cell lysate) and exposed manganese (amount put into the cell culture dish, 20 mg kg⁻¹). In addition to measuring the exposed amount of particles (uptake), we also tried to estimate characteristics of agglomeration and their influence on the dose delivered to the cell using the computational approach described by Cohen et al.²⁸ to facilitate a comparison to existing methodologies (**Supplementary Figure S6**).

In the cell lysate, the concentration of metals is a result of uptake of particles and dissolved metal (only in the case of manganese). Overall, significant amounts of metal were taken up in the cells (the cell volume is much smaller than the liquid volume in a typical in vitro experiment, hence, the intracellular metal concentrations are elevated). Also in cell lysates, accurate quantification of titania was impossible using the applied protocol. The measured uptake of ceria and manganese, though, confirm correct exposure, and stay in line with standard kinetics observed for oxide nanoparticle uptake into in vitro cultures²⁷. The continued uptake of manganese in macrophages, though, is in line with this cell's role in particle clearance²⁹. The slight decrease in manganese concentration observed after 24 hours may indicate partial detoxification of manganese, but needs further investigation in separate studies. The same applies for the time-dependent decrease of cerium in lysates of AEC, which has to be addressed in on-going investigations.

ROS-mediated decrease in viability of macrophages. Only marginal ROS formation in MAC and AEC was found in response to CeO₂ and TiO₂ particle exposure which is in good accordance with the results of Xia et al. in BEAS-2B and RAW 264.7 cells³⁰, as well as with in vivo findings in the bronchoalveolar lavage fluids of particle-exposed rats³¹. Exposure to

Mn₃O₄ particles induced a remarkable increase of ROS in MAC and provoked at the same time an impaired viability. No such an effect was found in AEC. This decrease in viability in MAC was accompanied by an elevation of caspase-3 activity, which suggests that particle-induced cell death is partly mediated by apoptosis. Addition of the free radical scavenger trolox alleviated Mn₃O₄-induced decrease in NADPH oxidase-related metabolic activity in MAC, however only partially. This indicates that oxidative stress together with other mechanisms contributes to decreased cell viability. Several previous studies have shown that particle-induced oxidative stress in human lung epithelial cell lines may exert cytotoxicity via apoptosis^{1, 32}. In our study, however, no cytotoxic effect of the three metal oxide particles in AEC was observed. The difference between the two cell lines MAC and AEC with regard to ROS formation and changes in cell viability in response to particle exposure may be explained by the fact that MAC possess more lysosomes than AEC. A disruption of a larger quantity of lysosomes in MAC compared to AEC after intracellular dissolution of Mn₃O₄ particles³³ may result in higher oxidative stress provoking decreased metabolic activity and suppressing inflammatory mediator secretion. Even insoluble particles might produce ROS formation in macrophages, which would be just a natural mechanism to try to destroy or kill everything what has been phagocytized.

Attenuated inflammatory mediator expression in response to oxidative stress. An up-regulation of several inflammatory mediators (interleukin-6, IL-6; IL-8; macrophage inflammatory protein-1 β , MIP-1 β ; MCP-1) in response to TiO₂ particle exposure is described in vitro (neutrophils, A549 cells) and in vivo^{32, 34-36}. We therefore expected to measure a pro-inflammatory response – in accordance with the increased intracellular ROS levels. In contrast to others, we did not observe raised inflammatory mediator levels in AEC. In MAC an even decreased MCP-1 protein expression after exposure to Mn₃O₄ particles was detected. To elucidate whether the measured attenuation of inflammatory mediator expression is due to oxidative cell damage / intracellular stress by Mn₃O₄ particles, we performed experiments

with a free radical scavenger. The Mn_3O_4 -induced suppression of MCP-1 protein secretion in MAC could be completely reversed by addition of trolox to the culture medium, which confirmed that oxidative stress attenuated inflammatory mediator production. In AEC, a decreased expression of MCP-1 protein was observed in response to CeO_2 particle exposure – though independent from intracellular ROS levels. One may speculate the decreased inflammatory mediator production to be the result of intracellular stress triggered through mechanisms of initial nanoparticle detoxification (e.g. enclosing CeO_2 particles in vesicles) ²⁰. Other studies, however, describe cytoprotective effects and attenuated inflammation in response to ceria nanostructures ³⁷⁻⁴⁰. In the present study, the molecular crosslink between particle-induced production of ROS and MCP-1 remains unknown. We demonstrated that the effects in MAC are trolox-sensitive, but only can speculate that ROS-induced modified activity of several protein kinases regulating inflammatory pathways might cause the measured changes in MCP-1 expression ⁴¹. It has certainly to be mentioned that the influence of antioxidants already present in cells and epithelial lining fluid (glutathione, ascorbate, uric acid) might play an important role in the modification of the inflammatory response ¹¹. In addition, MAC and AEC were observed under in vitro conditions using rat cell lines, which do not accurately mimic the conditions in a living organism. There are also other in vitro approaches using an air-liquid interface (with nebulization of the nanoparticles) which might simulate a more realistic particle exposure scenario ⁴². Secretion of MCP-1 protein, but not of CINC-1 and $\text{TNF-}\alpha$ protein was in the detection range of the ELISAs which represents another limitation of the used experimental approaches. In conclusion, this study assessed the response of two cell-types of the respiratory compartment on exposure to three, well-characterized metal oxides with regard to their intracellular solubility and redox-activity. We show that redox-active, soluble Mn_3O_4 particles compromise cell viability and decrease expression of inflammatory mediator in MAC partially mediated through a ROS-dependent mechanism. Interestingly, this type of nanomaterial only marginally triggered ROS formation

in AEC. Alveolar macrophages do not respond to an incubation with the redox-active, insoluble metal oxide CeO₂, while AEC show impaired viability and decreased production of inflammatory mediators, however ROS-independent. Finally the data revealed that each cell type reacts in a different way to metal oxide nanoparticle exposure making a prediction of the response depending from redox activity and intracellular solubility difficult.

FIGURES

Figure 1. X-ray diffraction patterns of nanoparticles. TiO₂ nanoparticles consist of rutile and anatase phases, CeO₂ and Mn₃O₄ consist of single phases (A). TEM images of Mn₃O₄ particles before (B) and after incubation for 4h in the cell medium with rat macrophages (C). Traces of metals according to ICP-OES measurements in the cell lysates of macrophages (D) and epithelial cells (E) shown in mg kg⁻¹ medium. Values for titanium are not shown as they were below the limit of detection (2 ppb).

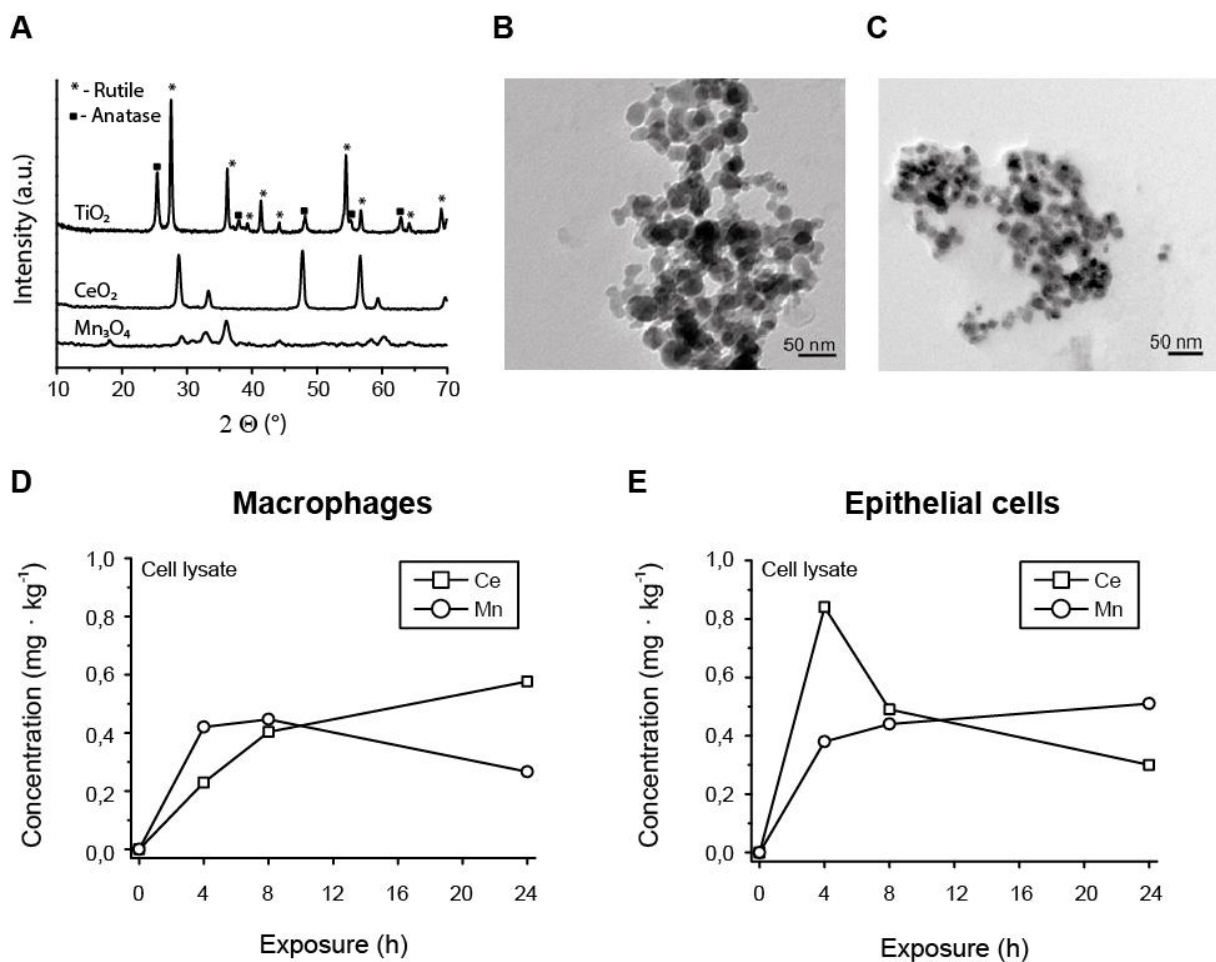


Figure 2. To detect generation of intracellular formation of reactive oxygen species (ROS), macrophages (MAC) (A) as well as alveolar epithelial cells (AEC) (B) were incubated with DCFH-DA and subsequently exposed to the different metal oxide particles. ROS levels as indicated by the increase in DCF fluorescence were determined as function of time. The potent ROS-stimulator SIN-1 was used as positive control at a concentration of 200 μ M. Levels in unexposed control cells were defined as 100%. Values are presented as mean \pm standard deviation.

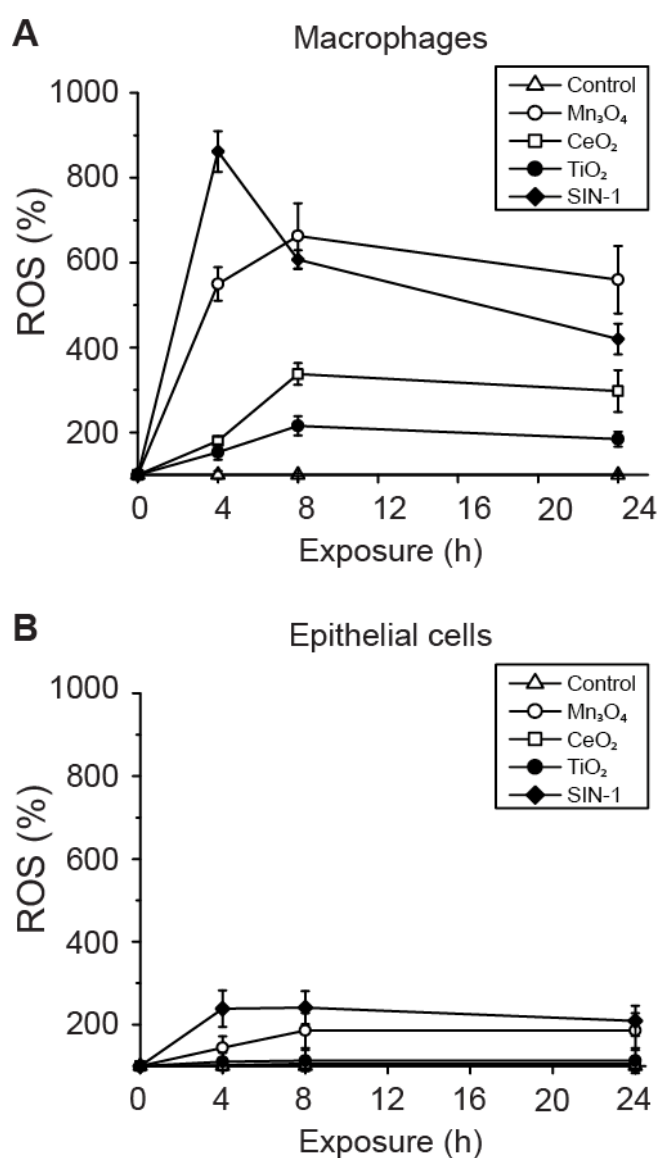


Figure 3. NADPH oxidase-related metabolic activity (MTT, metabolic activity) was measured in alveolar macrophages (MAC) (A). Demonstration of dose-dependent attenuation of MTT in MAC after exposure to manganese oxide particles (B). NADPH oxidase-related metabolic activity in alveolar epithelial cells (AEC) (C). Demonstration of dose-dependent attenuation of MTT in AEC after exposure to cerium oxide particles (D). Control was defined as 100%. In bar plots, values are shown as mean \pm SD.

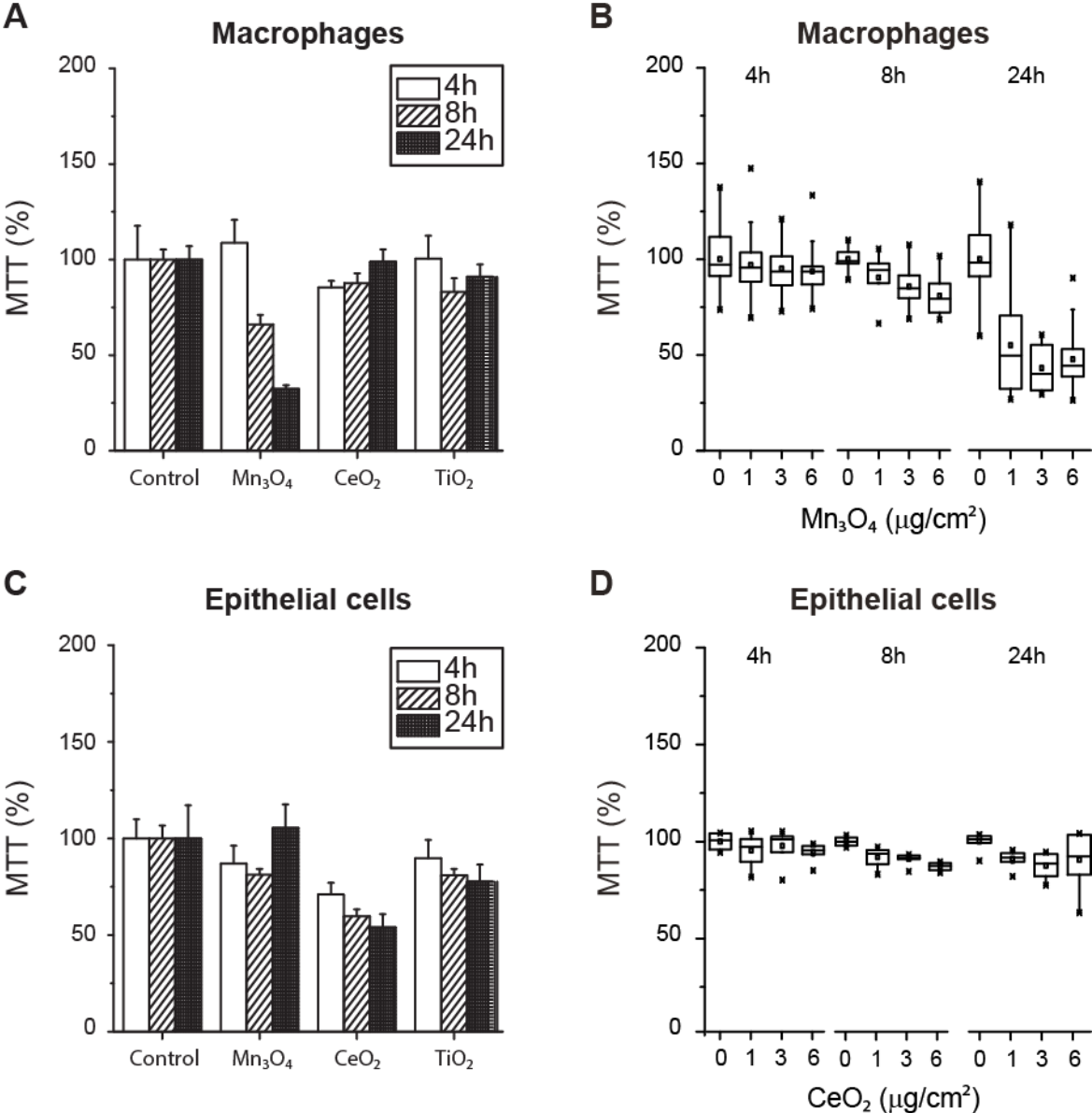


Figure 4. Monocyte chemoattractant protein-1 (MCP-1) expression as marker of inflammatory response was determined in alveolar macrophages (MAC) after exposure to the three nanoparticles ($6\mu\text{g}/\text{cm}^2$ cell surface) (A). MCP-1 protein expression in MAC after exposure to different Mn_3O_4 concentrations (B). Expression of MCP-1 in alveolar epithelial cells (AEC) was assessed as well upon incubation with the three particles ($6\mu\text{g}/\text{cm}^2$ cell surface) (C). MCP-1 protein expression in AEC after exposure to different CeO_2 concentrations (D). Control was defined as 100%.

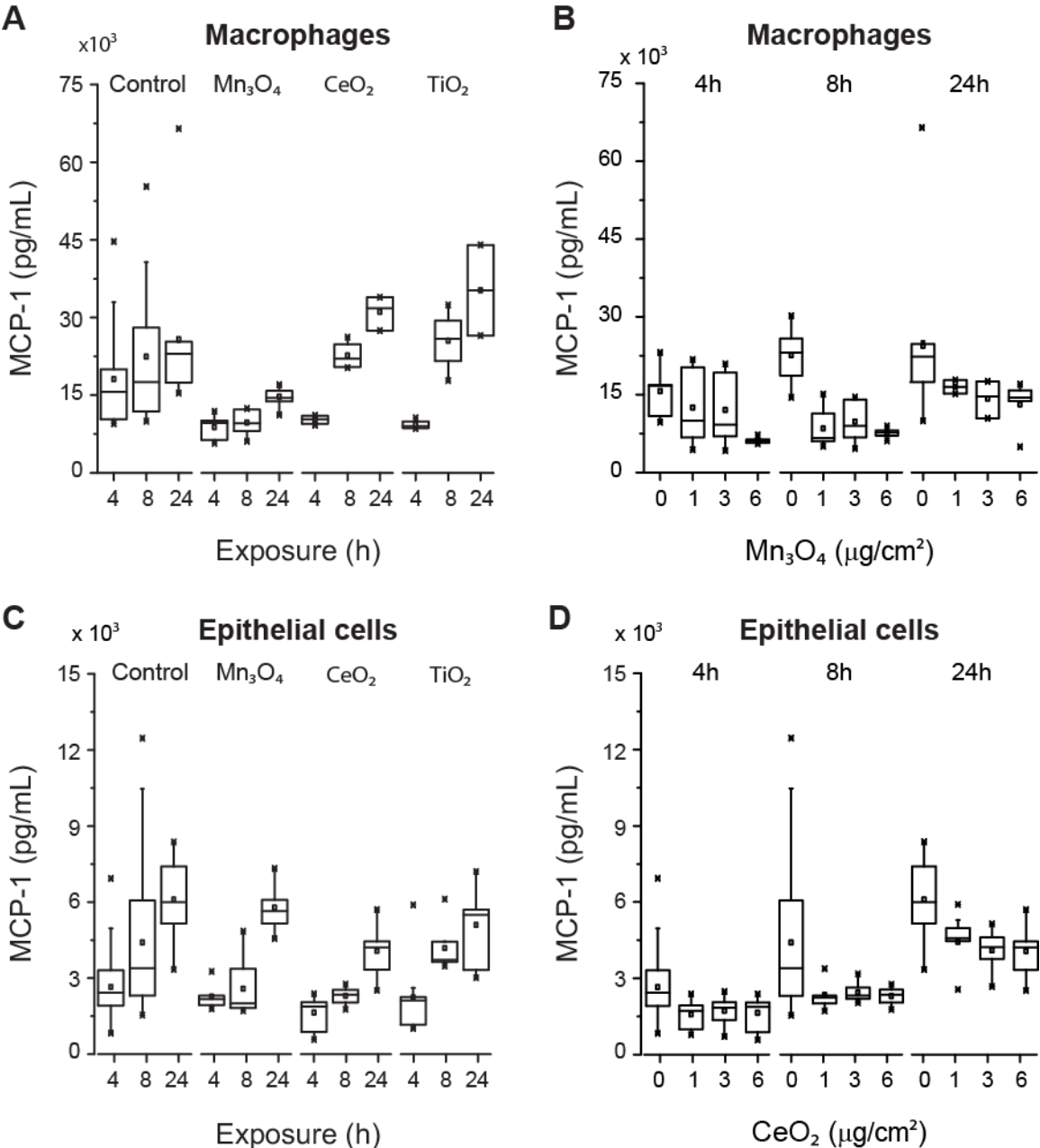
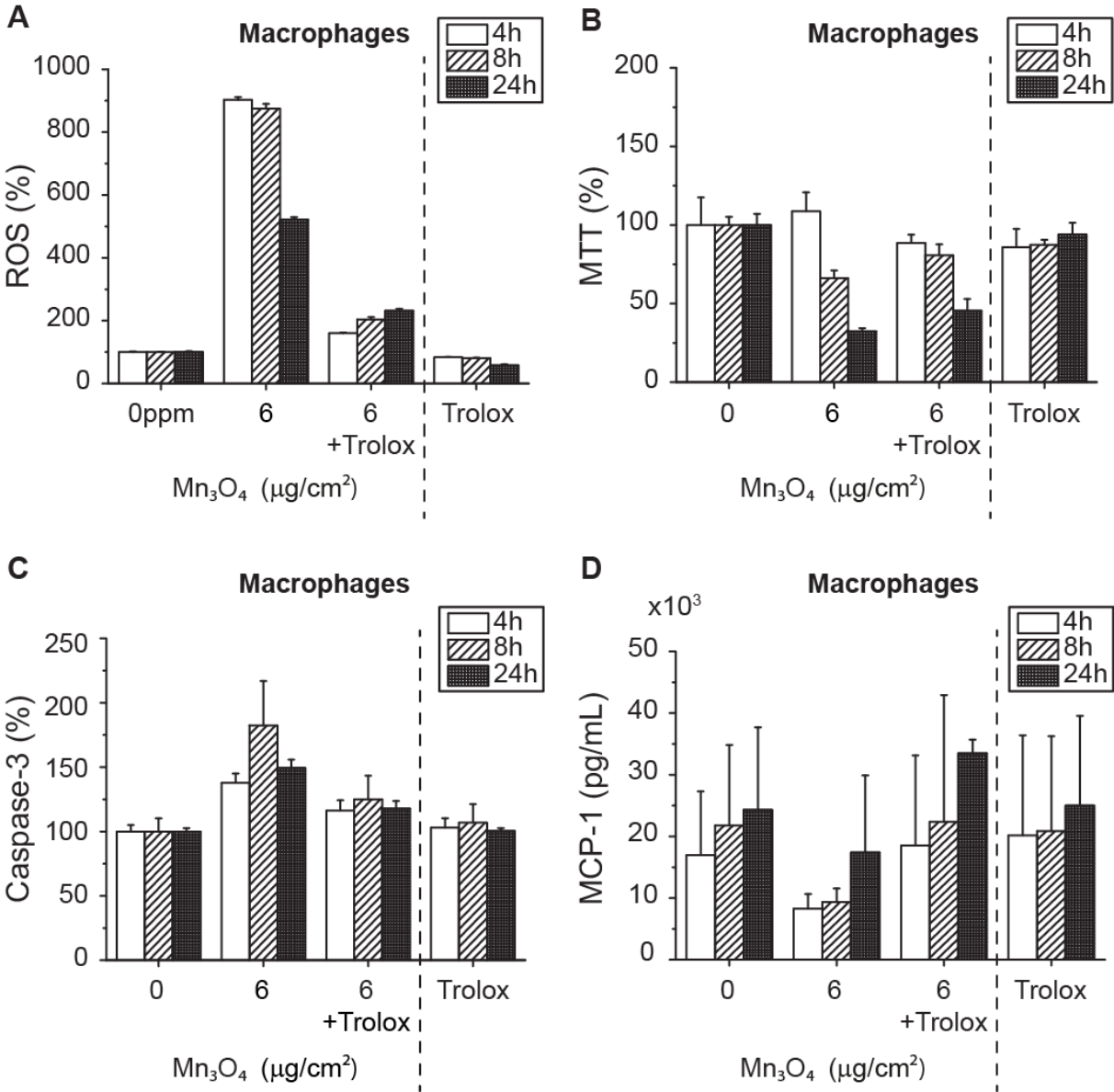


Figure 5. Mechanism of impaired viability and attenuated inflammatory mediator secretion in alveolar macrophages (MAC). The influence of manganese oxide particle (Mn_3O_4) exposure was evaluated in the presence of trolox (a derivative of vitamin E) as an antioxidant. Formation of reactive oxygen species (ROS) (A). Determination of NADPH oxidase-related metabolic activity (MTT, metabolic activity) (B). Activity of caspase-3 as marker of apoptosis (C). Monocyte chemoattractant protein-1 (MCP-1) expression (D). Control was defined as 100%. Values are presented as mean \pm SD.



ASSOCIATED CONTENT

Supporting Information. More details on materials and methods, as well as additional figures and tables are contained in the supplementary information of this article. This material is available free of charge via the Internet at <http://pubs.acs.org>.

AUTHOR INFORMATION

Corresponding Author

* Beatrice Beck-Schimmer, M.D., Institute of Physiology and Centre for Integrative Human Physiology, University of Zurich, Winterthurerstrasse 190, CH-8057 Zurich, Switzerland; Phone: +41 44 635 50 35, Fax: +41 44 635 68 14; E-mail: beatrice.beckschimmer@uzh.ch

Author Contributions

The manuscript was written through contributions of all authors. All authors have given approval to the final version of the manuscript. ‡ These authors contributed equally as first authors. X These authors contributed equally as senior authors. B.B.S., L.K.L., M.U. and W.J.S. designed the research. A.S., B.R.Z., C.B., K.P.B., A.ST., and M.U. performed the experimental research, C.C. and M.U. the statistical analysis. A.S., B.B.S., B.R.Z., A.ST., and M.U. wrote the paper.

Funding Sources

This work was supported by the Stiftung für Staublungenforschung, Switzerland and by private funding, administered by UBS, Zurich, Switzerland. The funders had no role in study design, data collection and analysis, decision to publish, or preparation of the manuscript.

ACKNOWLEDGMENT

We thank Ramon Frick for support for determination of reactive oxygen species. We thank Melanie Hasler and Livia Reyes for technical support.

REFERENCES

1. Lin, W.; Huang, Y. W.; Zhou, X. D.; Ma, Y., Toxicity of cerium oxide nanoparticles in human lung cancer cells. *Int J Toxicol* **2006**, *25*, (6), 451-7.
2. Kaida, T.; Kobayashi, K.; Adachi, M.; Suzuki, F., Optical characteristics of titanium oxide interference film and the film laminated with oxides and their applications for cosmetics. *J Cosmet Sci* **2004**, *55*, (2), 219-20.
3. Bader, M.; Dietz, M. C.; Ihrig, A.; Triebig, G., Biomonitoring of manganese in blood, urine and axillary hair following low-dose exposure during the manufacture of dry cell batteries. *Int Arch Occup Environ Health* **1999**, *72*, (8), 521-7.
4. Iregren, A., Manganese neurotoxicity in industrial exposures: Proof of effects, critical exposure level, and sensitive tests. *Neurotoxicology* **1999**, *20*, (2-3), 315-323.
5. Sferlazza, S. J.; Beckett, W. S., The respiratory health of welders. *Am Rev Respir Dis* **1991**, *143*, (5 Pt 1), 1134-48.
6. Antonini, J. M.; Lewis, A. B.; Roberts, J. R.; Whaley, D. A., Pulmonary effects of welding fumes: review of worker and experimental animal studies. *Am J Ind Med* **2003**, *43*, (4), 350-60.
7. Ahsan, S. A.; Lackovic, M.; Katner, A.; Palermo, C., Metal fume fever: a review of the literature and cases reported to the Louisiana Poison Control Center. *J La State Med Soc* **2009**, *161*, (6), 348-51.

8. Wergeland, E.; Iversen, B. G., Deaths from pneumonia after welding. *Scand J Work Environ Health* **2001**, *27*, (5), 353.
9. Palmer, K. T.; Cullinan, P.; Rice, S.; Brown, T.; Coggon, D., Mortality from infectious pneumonia in metal workers: a comparison with deaths from asthma in occupations exposed to respiratory sensitisers. *Thorax* **2009**, *64*, (11), 983-6.
10. Limbach, L. K.; Wick, P.; Manser, P.; Grass, R. N.; Bruinink, A.; Stark, W. J., Exposure of engineered nanoparticles to human lung epithelial cells: influence of chemical composition and catalytic activity on oxidative stress. *Environ Sci Technol* **2007**, *41*, (11), 4158-63.
11. Frick, R.; Muller-Edenborn, B.; Schlicker, A.; Rothen-Rutishauser, B.; Raemy, D. O.; Gunther, D.; Hattendorf, B.; Stark, W.; Beck-Schimmer, B., Comparison of manganese oxide nanoparticles and manganese sulfate with regard to oxidative stress, uptake and apoptosis in alveolar epithelial cells. *Toxicol Lett* **2011**, *205*, (2), 163-72.
12. Demou, E.; Stark, W. J.; Hellweg, S., Particle Emission and Exposure during Nanoparticle Synthesis in Research Laboratories. *Annals of Occupational Hygiene* **2009**, *53*, (8), 829-838.
13. Steurer, M.; Schlapfer, M.; Steurer, M.; Z'Graggen B, R.; Booy, C.; Reyes, L.; Spahn, D. R.; Beck-Schimmer, B., The volatile anaesthetic sevoflurane attenuates lipopolysaccharide-induced injury in alveolar macrophages. *Clin Exp Immunol* **2009**, *155*, (2), 224-30.
14. Suter, D.; Spahn, D. R.; Blumenthal, S.; Reyes, L.; Booy, C.; Z'Graggen B, R.; Beck-Schimmer, B., The immunomodulatory effect of sevoflurane in endotoxin-injured alveolar epithelial cells. *Anesth Analg* **2007**, *104*, (3), 638-45.

15. Foucaud, L.; Wilson, M. R.; Brown, D. M.; Stone, V., Measurement of reactive species production by nanoparticles prepared in biologically relevant media. *Toxicol Lett* **2007**, *174*, (1-3), 1-9.
16. Wang, H.; Joseph, J. A., Quantifying cellular oxidative stress by dichlorofluorescein assay using microplate reader. *Free Radic Biol Med* **1999**, *27*, (5-6), 612-6.
17. Volk, T.; Ioannidis, I.; Hensel, M.; deGroot, H.; Kox, W. J., Endothelial damage induced by nitric oxide: synergism with reactive oxygen species. *Biochem Biophys Res Commun* **1995**, *213*, (1), 196-203.
18. Mosmann, T., Rapid colorimetric assay for cellular growth and survival: application to proliferation and cytotoxicity assays. *J Immunol Methods* **1983**, *65*, (1-2), 55-63.
19. Labarca, C.; Paigen, K., A simple, rapid, and sensitive DNA assay procedure. *Analytical Biochemistry* **1980**, *102*, (2), 344-52.
20. Brunner, T. J.; Wick, P.; Manser, P.; Spohn, P.; Grass, R. N.; Limbach, L. K.; Bruinink, A.; Stark, W. J., In vitro cytotoxicity of oxide nanoparticles: comparison to asbestos, silica, and the effect of particle solubility. *Environ Sci Technol* **2006**, *40*, (14), 4374-81.
21. Z'Graggen B, R.; Tornic, J.; Muller-Edenborn, B.; Reyes, L.; Booy, C.; Beck-Schimmer, B., Acute lung injury: apoptosis in effector and target cells of the upper and lower airway compartment. *Clin Exp Immunol* **2010**, *161*, (2), 324-31.
22. Howard, P.; Billings, C. G., Dynamics and clinical effects of nonferrous metals in the human body. *Monaldi Arch Chest Dis* **2000**, *55*, (1), 70-3.
23. Boojar, M. M.; Goodarzi, F., A longitudinal follow-up of pulmonary function and respiratory symptoms in workers exposed to manganese. *J Occup Environ Med* **2002**, *44*, (3), 282-90.

24. Zhang, H. Y.; Ji, Z. X.; Xia, T.; Meng, H.; Low-Kam, C.; Liu, R.; Pokhrel, S.; Lin, S. J.; Wang, X.; Liao, Y. P.; Wang, M. Y.; Li, L. J.; Rallo, R.; Damoiseaux, R.; Telesca, D.; Madler, L.; Cohen, Y.; Zink, J. I.; Nel, A. E., Use of Metal Oxide Nanoparticle Band Gap To Develop a Predictive Paradigm for Oxidative Stress and Acute Pulmonary Inflammation. *Acs Nano* **2012**, *6*, (5), 4349-4368.
25. Cronholm, P.; Karlsson, H. L.; Hedberg, J.; Lowe, T. A.; Winnberg, L.; Elihn, K.; Wallinder, I. O.; Moller, L., Intracellular uptake and toxicity of Ag and CuO nanoparticles: a comparison between nanoparticles and their corresponding metal ions. *Small* **2013**, *9*, (7), 970-82.
26. Semisch, A.; Ohle, J.; Witt, B.; Hartwig, A., Cytotoxicity and genotoxicity of nano - and microparticulate copper oxide: role of solubility and intracellular bioavailability. *Part Fibre Toxicol* **2014**, *11*, 10.
27. Limbach, L. K.; Li, Y.; Grass, R. N.; Brunner, T. J.; Hintermann, M. A.; Muller, M.; Gunther, D.; Stark, W. J., Oxide nanoparticle uptake in human lung fibroblasts: effects of particle size, agglomeration, and diffusion at low concentrations. *Environ Sci Technol* **2005**, *39*, (23), 9370-6.
28. Cohen, J. M.; Teeguarden, J. G.; Demokritou, P., An integrated approach for the in vitro dosimetry of engineered nanomaterials. *Part Fibre Toxicol* **2014**, *11*, 20.
29. Geiser, M., Update on Macrophage Clearance of Inhaled Micro- and Nanoparticles. *Journal of Aerosol Medicine and Pulmonary Drug Delivery* **2010**, *23*, (4), 207-217.
30. Xia, T.; Kovoichich, M.; Liong, M.; Madler, L.; Gilbert, B.; Shi, H.; Yeh, J. I.; Zink, J. I.; Nel, A. E., Comparison of the mechanism of toxicity of zinc oxide and cerium oxide

nanoparticles based on dissolution and oxidative stress properties. *ACS Nano* **2008**, *2*, (10), 2121-34.

31. Dick, C. A.; Brown, D. M.; Donaldson, K.; Stone, V., The role of free radicals in the toxic and inflammatory effects of four different ultrafine particle types. *Inhal Toxicol* **2003**, *15*, (1), 39-52.

32. Park, E. J.; Yi, J.; Chung, K. H.; Ryu, D. Y.; Choi, J.; Park, K., Oxidative stress and apoptosis induced by titanium dioxide nanoparticles in cultured BEAS-2B cells. *Toxicol Lett* **2008**, *180*, (3), 222-9.

33. Studer, A. M.; Limbach, L. K.; Van Duc, L.; Krumeich, F.; Athanassiou, E. K.; Gerber, L. C.; Moch, H.; Stark, W. J., Nanoparticle cytotoxicity depends on intracellular solubility: comparison of stabilized copper metal and degradable copper oxide nanoparticles. *Toxicol Lett* **2010**, *197*, (3), 169-74.

34. Monteiller, C.; Tran, L.; MacNee, W.; Faux, S.; Jones, A.; Miller, B.; Donaldson, K., The pro-inflammatory effects of low-toxicity low-solubility particles, nanoparticles and fine particles, on epithelial cells in vitro: the role of surface area. *Occup Environ Med* **2007**, *64*, (9), 609-15.

35. Singh, S.; Shi, T.; Duffin, R.; Albrecht, C.; van Berlo, D.; Hohr, D.; Fubini, B.; Martra, G.; Fenoglio, I.; Borm, P. J.; Schins, R. P., Endocytosis, oxidative stress and IL-8 expression in human lung epithelial cells upon treatment with fine and ultrafine TiO₂: role of the specific surface area and of surface methylation of the particles. *Toxicology and Applied Pharmacology* **2007**, *222*, (2), 141-51.

36. Goncalves, D. M.; Chiasson, S.; Girard, D., Activation of human neutrophils by titanium dioxide (TiO₂) nanoparticles. *Toxicol In Vitro* **2010**, *24*, (3), 1002-8.

37. Hirst, S. M.; Karakoti, A. S.; Tyler, R. D.; Sriranganathan, N.; Seal, S.; Reilly, C. M., Anti-inflammatory properties of cerium oxide nanoparticles. *Small* **2009**, *5*, (24), 2848-56.
38. Chen, J.; Patil, S.; Seal, S.; McGinnis, J. F., Rare earth nanoparticles prevent retinal degeneration induced by intracellular peroxides. *Nat Nanotechnol* **2006**, *1*, (2), 142-50.
39. Schubert, D.; Dargusch, R.; Raitano, J.; Chan, S. W., Cerium and yttrium oxide nanoparticles are neuroprotective. *Biochemical and Biophysical Research Communications* **2006**, *342*, (1), 86-91.
40. Tarnuzzer, R. W.; Colon, J.; Patil, S.; Seal, S., Vacancy engineered ceria nanostructures for protection from radiation-induced cellular damage. *Nano Lett* **2005**, *5*, (12), 2573-7.
41. Griendling, K. K.; Sorescu, D.; Lassegue, B.; Ushio-Fukai, M., Modulation of protein kinase activity and gene expression by reactive oxygen species and their role in vascular physiology and pathophysiology. *Arterioscler Thromb Vasc Biol* **2000**, *20*, (10), 2175-83.
42. Lenz, A. G.; Karg, E.; Lentner, B.; Dittrich, V.; Brandenberger, C.; Rothen-Rutishauser, B.; Schulz, H.; Ferron, G. A.; Schmid, O., A dose-controlled system for air-liquid interface cell exposure and application to zinc oxide nanoparticles. *Part Fibre Toxicol* **2009**, *6*, 32.